J|A|C|S ARTICLES

Published on Web 12/14/2009

Thermal Decomposition Mechanism of Single-Molecule Precursors Forming Metal Sulfide Nanoparticles

Yun Ku Jung, Jae Il Kim, and Jin-Kyu Lee*

Department of Chemistry, Seoul National University, Seoul 151-747, South Korea

Received July 10, 2009; E-mail: jinklee@snu.ac.kr

Abstract: Several zinc alkyldithiocarbamates [$Zn(S_2CNR_2)_2$] were synthesized, and their thermal decomposition in the presence of alkylamines was studied in order to understand the formation of metal sulfide nanoparticles. The major intermediates and side products were isolated under various conditions and characterized by NMR spectroscopy and LC−MS. The analysis results showed that nucleophilic attack of the metal-coordinated amine on the most electron-deficient thiocarbonyl carbon of the alkyldithiocarbamate ligands at high temperature initiated the decomposition to generate thiourea, hydrogen sulfide, and solid metal sulfide nanoparticles. From the proposed decomposition mechanism, the role of amines in thermolysis was studied, and methods for synthesizing various metal sulfide nanoparticles were generalized. Formation of the desired products was confirmed by carrying out model experiments.

Introduction

Because of their unique properties and potential applications, nanoparticles have been extensively studied by several research groups. Thermal decomposition (i.e., thermolysis or pyrolysis) of organometallic precursors is the representative method of nanoparticle synthesis. Thermal decomposition allows easier and simpler control of the shapes and sizes of the nanoparticles than do other methods. In the past decade, many research groups have investigated the synthesis and characterization of nanoparticles of various compositions, sizes, shapes, and properties.[1−4]

Because of their size-dependent optical and electrical properties, semiconductor quantum dots (QDs) have attracted the attention of researchers.[3] Since Bawendi and co-workers[5] synthesized metal chalcogenide QDs (which first showed band-edge emission at room temperature) by carrying out high-temperature pyrolysis of the organometallic and chalcogenide precursors in a coordinating solvent, extensive research on the synthesis and characterization of QDs has been carried out. Peng and Peng[6] developed a new method of metal chalcogenide QD synthesis using cadmium oxide and phosphonic acid, which dramatically resolved a safety issue with respect to materials, but high temperature was required for thermal decomposition. Hence, the use of single-molecule precursors for the synthesis of QDs was proposed,[7−11] and has been reported that primary amines promote nanoparticle formation at low temperatures.[12,13] Recently, metal dialkyldithiocarbamates have been used as a single-molecule source for the synthesis of semiconductor QDs and rare-earth metal sulfide nanoparticles.[8,9,14−16] Zinc diethylthiocarbamate [$Zn(DETC)_2$] has also been used as a single-molecule source for QD synthesis; in this method, ZnS shells are grown around the surface of CdSe QDs in a microfluidic system.[17] The growth kinetics and shape evolution of the nanoparticles synthesized by thermolysis have been actively studied. However, the role of the amine in nanoparticle synthesis and the exact mechanism of conversion of the precursor molecules into intermediates and the subsequent decomposition of the intermediates into nanoparticles have not been investigated in detail.[18−23]

Metal dialkyldithiocarbamates have been widely used as active accelerators in the sulfur vulcanization of rubber[24] and

(1) Cushing, B. L.; Kolesnichenko, V. L.; O'Connor, C. J. *Chem. Rev.* **2004**, *104*, 3893–3946.
(2) Yin, Y.; Alivisatos, A. P. *Nature* **2005**, *437*, 664–670.
(3) Alivisatos, A. P. *J. Phys. Chem.* **1996**, *100*, 13226–13239.
(4) Lu, A.-H.; Salabas, E. L.; Schüth, F. *Angew. Chem., Int. Ed.* **2007**, *46*, 1222–1244.
(5) Murray, C. B.; Norris, D. J.; Bawendi, M. G. *J. Am. Chem. Soc.* **1993**, *115*, 8706–8715.
(6) Peng, Z. A.; Peng, X. *J. Am. Chem. Soc.* **2001**, *123*, 183–184.
(7) Trindade, T.; O'Brien, P. *Adv. Mater.* **1996**, *8*, 161–163.
(8) Trindade, T.; O'Brien, P.; Zhang, X.-m. *Chem. Mater.* **1997**, *9*, 523–530.
(9) Trindade, T.; OBrien, P.; Zhang, X.-m.; Motevalli, M. *J. Mater. Chem.* **1997**, *7*, 1011–1016.
(10) Cumberland, S. L.; Hanif, K. M.; Javier, A.; Khitrov, G. A.; Strouse, G. F.; Woessner, S. M.; Yun, C. S. *Chem. Mater.* **2002**, *14*, 1576–1584.
(11) Pradhan, N.; Efrima, S. *J. Am. Chem. Soc.* **2003**, *125*, 2050–2051.
(12) Pradhan, N.; Katz, B.; Efrima, S. *J. Phys. Chem. B* **2003**, *107*, 13843–13854.
(13) Zhang, Z.; Lee, S. H.; Vittal, J. J.; Chin, W. S. *J. Phys. Chem. B* **2006**, *110*, 6649–6654.
(14) Trindade, T.; O'Brien, P. *J. Mater. Chem.* **1996**, *6*, 343–347.
(15) Lee, S.-M.; Jun, Y.-W.; Cho, S.-N.; Cheon, J. *J. Am. Chem. Soc.* **2002**, *124*, 11244–11245.
(16) Mirkovic, T.; Hines, M. A.; Nair, P. S.; Scholes, G. D. *Chem. Mater.* **2005**, *17*, 3451–3456.
(17) Wang, H.; Nakamura, H.; Uehara, M.; Yamaguchi, Y.; Miyazaki, M.; Maeda, H. *Adv. Funct. Mater.* **2005**, *15*, 603–608.
(18) Peng, X.; Wickham, J.; Alivisatos, A. P. *J. Am. Chem. Soc.* **1998**, *120*, 5343–5344.
(19) Manna, L.; Scher, E. C.; Alivisatos, A. P. *J. Am. Chem. Soc.* **2000**, *122*, 12700–12706.
(20) Peng, X.; Manna, L.; Yang, W.; Wickham, J.; Scher, E.; Kadavanich, A.; Alivisatos, A. P. *Nature* **2000**, *404*, 59–61.
(21) Manna, L.; Milliron, D. J.; Meisel, A.; Scher, E. C.; Alivisatos, A. P. *Nat. Mater.* **2003**, *2*, 382–385.
(22) Kanaras, A. G.; Sonnichsen, C.; Liu, H.; Alivisatos, A. P. *Nano Lett.* **2005**, *5*, 2164–2167.
(23) Kwon, S. G.; Hyeon, T. *Acc. Chem. Res.* **2008**, *41*, 1696–1709.

10.1021/ja905353a

as metal sulfide precursors in metal−organic chemical vapor deposition (MOCVD) applications.[25,26] This is because they are moisture-insensitive, air-stable, less toxic, and easy to synthesize and handle. Interestingly, Reedijk and co-workers[27] have proposed a mechanism for thermal decomposition of zinc dimethyldithiocarbamate to explain the cross-linking of *cis*-1,4-polybutadiene with a cyclic disulfide in the presence of zinc dimethylthiocarbamate [$Zn(DMTC)_2$] and a primary amine. They carried out a reaction between $Zn(DMTC)_2$ and hexylamine to explain the generation of hydrogen sulfide (H_2S), which helps in the cross-linking of the unsaturated rubbers. They observed the generation of dimethylamine (Me_2NH), H_2S, a solid ZnS precipitate, and asymmetric and symmetric thiourea by the thermolysis of $Zn(DMTC)_2$ with hexylamine and proposed several transition states generated by the interaction of coordinated hexylamine with the DMTC ligands. However, they focused on the generation of H_2S and proposed a decomposition mechanism on the basis of only the final decomposed products obtained in sealed-tube reaction systems.

Here we propose a new mechanism for the decomposition of $Zn(DMTC)_2$ in the presence of alkylamines on the basis of the results of studies conducted on the isolated intermediates and the side products obtained at 1 atm. In this mechanism, nucleophilic attack of the metal-coordinated amine on the most electron-deficient thiocarbonyl carbon of the alkyldithiocarbamate ligands at high temperature initiates the decomposition of $Zn(DMTC)_2$; steric hindrance in the alkylamine plays a very important role in the thermolysis. This reaction mechanism could be extended to other metal sulfide nanosystems and used as a good basis for the synthesis of high-quality metal sulfide and related nanoparticles.

Experimental Section

Chemicals and Instrumentation. $Zn(DMTC)_2$ was purchased from TCI. Zinc chloride ($ZnCl_2$), lead nitrate [$Pb(NO_3)_2$], sodium diethylthiocarbamate (NaDETC), octylamine (NH_2Oct), oleic acid, and the solvents (hexane, chloroform, toluene, and ethanol) were purchased from Aldrich. NMR solvents [toluene-d_8, dimethyl sulfoxide-d_6 (DMSO-d_6), and chloroform-d_1] were purchased from CIL. All of the chemicals were used as received without further purification. UV−vis spectra were recorded on a S-3100 spectrophotometer (Scinco). Powder X-ray diffraction (XRD) measurements were carried out on D8 Advance diffractometer (Bruker). Transmission electron microscopy (TEM) and energy-dispersive spectroscopy (EDS) were conducted using Hitachi-7600 (Hitachi) and JEM-3000F (JEOL) instruments, respectively. NMR spectra were recorded on NMR 500 (Varian) and DPX 300 (Bruker) spectrometers. Liquid chromatography−mass spectrometry (LC−MS) measurements were carried out using a Finnigan Surveyor MSQ LC/MS Plus instrument (Thermo Electron Corporation).

Synthesis of Zinc Sulfide. $Zn(DMTC)_2$ was used as a precursor for the synthesis of ZnS nanoparticles. $Zn(DMTC)_2$ was mixed with an appropriate amount of octylamine in toluene, and the solution was heated to 100 °C and maintained at this temperature. The gas evolved during heating was trapped by an aqueous Pb^{2+} solution. Next, the reaction mixture was cooled to room temperature and then centrifuged to separate the organic side products and the solid precipitate. The organic side products were characterized by LC−MS and NMR spectroscopy after the solvent was removed in vacuo. The solid precipitate was characterized by TEM and XRD.

In Situ Monitoring of Thermal Decomposition. A colorless toluene solution containing $Zn(DMTC)_2$ and an appropriate amount of octylamine was heated at 50 °C and then cooled to room temperature, after which the solution was centrifuged to separate $Zn(DMTC)_2 \cdot 2NH_2Oct$. The isolated $Zn(DMTC)_2 \cdot 2NH_2Oct$ was dissolved in DMSO-d_6 and analyzed by variable-temperature NMR (VT-NMR) spectroscopy. Using the NMR heating system, the solution was heated for 30 min from 60 to 100 °C in intervals of 10 °C to achieve thermal equilibrium.

Synthesis of Sodium Octyldithiocarbamate ($NaS_2CNHOct$). $NaS_2CNHOct$ was prepared using a slightly modified version of the method reported in the literature.[28] To the preheated aqueous solution of 0.01 mol of octylamine and an equimolar amount of NaOH at 100 °C, 25 mL of toluene containing 0.012 mol of carbon disulfide was added dropwise with cooling and vigorous stirring. The reaction mixture was stirred for 1 h, diluted with 100 mL of petroleum ether, and then stirred for an additional 2 h. The mixture was filtered on a sintered glass funnel, and the residue was washed with petroleum ether and dried to obtain the pure of $NaS_2CNHOct$ (1.78 g; 82.7% yield).

Synthesis of Zinc Octyldithiocarbamate [$Zn(S_2CNHOct)_2$]. $Zn(S_2CNHOct)_2$ was synthesized using the method reported in the literature.[8] Equimolar amounts of aqueous $ZnCl_2$ and $NaS_2CNHOct$ solutions were mixed and stirred for 10 min. The precipitate was filtered, washed with a large amount of distilled water, and dried in air to obtain $Zn(S_2CNHOct)_2$ (90.6% yield). ^{1}H NMR (300 MHz, DMSO-d_6): δ 9.95 (br s, −N*H*−, 2H), 3.29 (q, −NHCH_2−, 4H), 1.50 (m, −CH_2CH_2−, 4H), 1.25 (s, −C_5H_{10}−, 20H), 0.85 (t, −CH_3, 6H).

Thermal Decomposition of $Zn(S_2CNHOct)_2$ in the Presence of Secondary Amine. $Zn(S_2CNHOct)_2$ was mixed with 2 equiv of dioctylamine in toluene, and the solution was heated to 100 °C. The gaseous and solid products as well as the organic side products were characterized as described previously.

Synthesis of Cadmium Diethyldithiocarbamate [$Cd(DETC)_2$]. $Cd(DETC)_2$ was synthesized using the method reported in the literature.[8] Equimolar amounts of aqueous $CdCl_2$ and Na(DETC) solutions were mixed and stirred for 10 min. The precipitate was filtered, washed with a large amount of distilled water, and dried in air to obtain $Cd(DETC)_2$ (89.5% yield). ^{1}H NMR (300 MHz, DMSO-d_6): δ 3.74 (m, −CH_2−, 8H), 1.22 (s, −CH_3, 12H).

Synthesis of Lead Diethyldithiocarbamate [$Pb(DETC)_2$]. $Pb(DETC)_2$ was prepared in a manner similar to that for the preparation of $Cd(DETC)_2$, which afforded the product in good yield (89%). ^{1}H NMR (300 MHz, DMSO-d_6): δ 3.74 (m, −CH_2−, 8H), 1.22 (s, −CH_3, 12H).

Synthesis of CdS and PbS Nanoparticles. The appropriate precursor complexes were mixed with 2 equiv of octylamine, and the solution was heated at 100 °C. The obtained nanoparticles were characterized in a manner similar to that described for the ZnS nanoparticles.

Results and Discussion

$Zn(DMTC)_2$ powder was mixed with 1 equiv of octylamine in toluene and heated at 50 °C to afford a homogeneous and colorless solution, which was then cooled to room temperature to obtain a white solid powder. The NMR spectrum of this solid in DMSO-d_6 showed representative peaks, including one at 2.74 ppm due to $NH_2-CH_2C_7H_{15}$ in the coordinated octylamine. The peaks observed in the spectrum matched well with those reported for the pentacoordinated $Zn(DMTC)_2 \cdot NH_2Oct$ complex, whose crystalline structure was also resolved by single-crystal X-ray

(24) Higgins, G. M. C.; Saville, B. *J. Chem. Soc.* **1963**, 2812–2817.
(25) Frigo, D. M.; Khan, O. F. Z.; O'Brien, P. *J. Cryst. Growth* **1989**, *96*, 989–992.
(26) Pike, R. D.; Cui, H.; Kershaw, R.; Dwight, K.; Wold, A.; Blanton, T. N.; Wernberg, A. A.; Gysling, H. J. *Thin Solid Films* **1993**, *224*, 221–226.
(27) Dirksen, A.; Nieuwenhuizen, P. J.; Hoogenraad, M.; Haasnoot, J. G.; Reedijk, J. *J. Appl. Polym. Sci.* **2001**, *79*, 1074–1083.
(28) Sawant, P.; Kovalev, E.; Klug, J. T.; Efrima, S. *Langmuir* **2001**, *17*, 2913–2917.

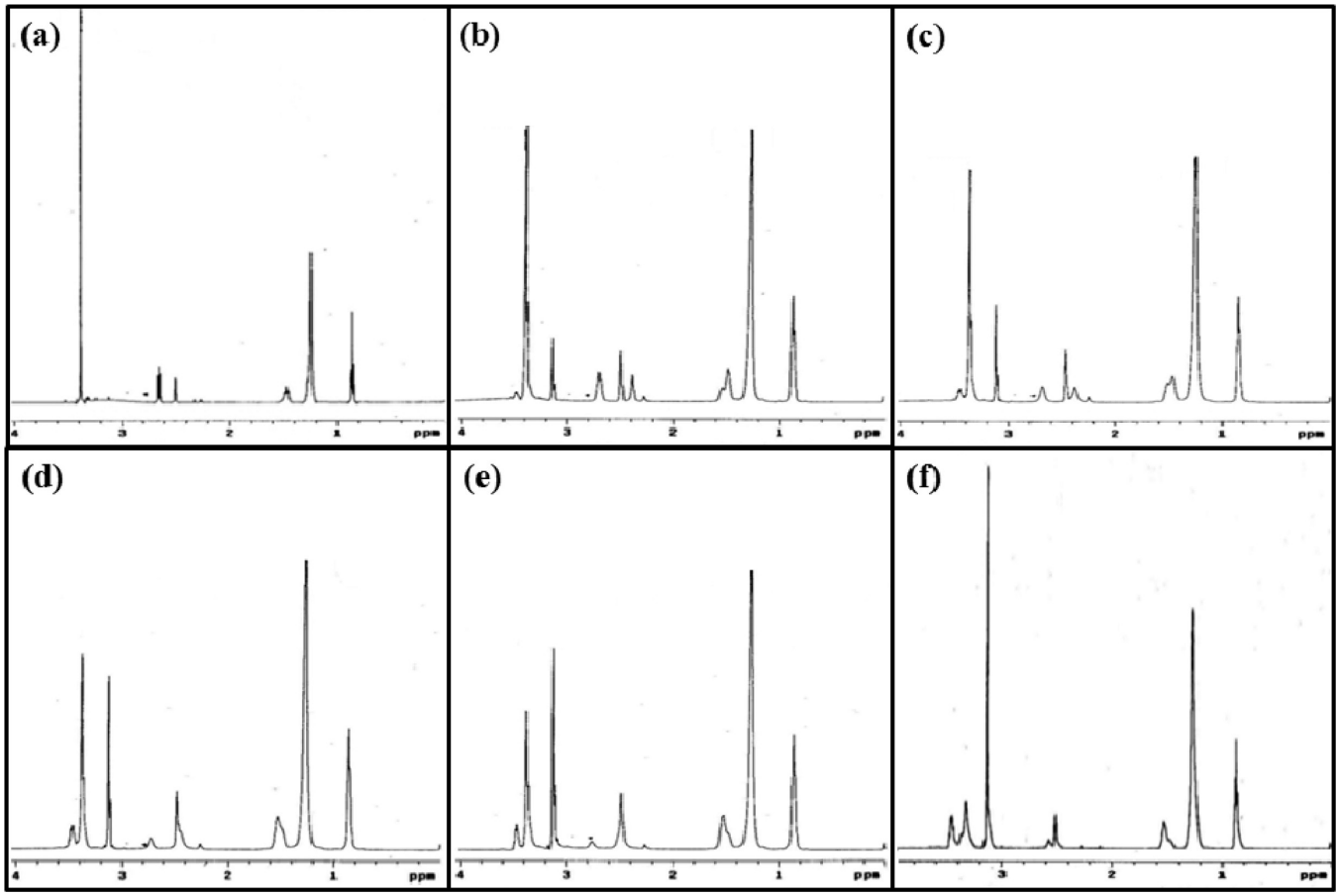

Figure 1. In situ NMR monitoring of the thermal decomposition of hexacoordinated $Zn(DMTC)_2 \cdot 2NH_2Oct$ at (a) 50, (b) 60, (c) 70, (d) 80, (e) 90, and (f) 100 °C.

crystallography. When $Zn(DMTC)_2$ was mixed with 2 equiv of octylamine, a waxy solid was obtained and confirmed by NMR analysis to be $Zn(DMTC)_2 \cdot 2NH_2Oct$. The NMR spectrum of this compound showed a peak due to $NH_2-CH_2C_7H_{15}$ at 2.66 ppm (Figure 1a); this δ value is between those for the free amine (2.53 ppm) and the pentacoordinated complex. All efforts to isolate the crystalline product to resolve the absolute configuration of $Zn(DMTC)_2 \cdot 2NH_2Oct$ were unsuccessful; this was probably a result of the weak interaction of the amines with the Zn metal site and the mixed structure of possible isomers. If more than 3 equiv of octylamine was mixed with $Zn(DMTC)_2$ or an excess amount of octylamine was added to the solution of $Zn(DMTC)_2 \cdot 2NH_2Oct$, only one peak at ~2.64 ppm, due to the $NH_2-CH_2C_7H_{15}$ group bound to Zn, was observed. The peak due to free $NH_2-CH_2C_7H_{15}$ was not observed. This confirmed that octylamine is not tightly bound to Zn in the solution but exists in a dynamic equilibrium state on NMR time scale. The instability of $Zn(DMTC)_2 \cdot 2NH_2Oct$ can be explained on the basis of this observation, which is supported by the fact that the structures of hexacoordinated compounds have been reported only in the case of chelating diamines such as bipyridine and phenanthroline.[29]

The isolated waxy solid of $Zn(DMTC)_2 \cdot 2NH_2Oct$ was dissolved in DMSO-d_6, and the changes in its structure were monitored using VT-NMR analysis. With an increase in temperature, all of the peaks in the spectrum broadened slightly. New peaks appeared at 3.44 and 3.12 ppm at 60 °C and became dominant at 100 °C (Figure 1b–f). For the analysis of the structural changes in the intermediates, the isolated $Zn(DMTC)_2 \cdot 2NH_2Oct$ was heated in toluene for 1 h at 100 °C. Subsequently, the solution was cooled to room temperature to obtain a white solid precipitate. The precipitate was dissolved in DMSO, and the tiny amount of insoluble material was removed by filtering through a 0.4 μm membrane filter; the solvent was then evaporated in vacuo. The spectrum of the solid residue showed peaks corresponding to $NH_2-CH_2C_7H_{15}$ and $-N(CH_3)_2$ at 3.47 and 3.12 ppm, respectively, in DMSO-d_6. From the integration ratios, the composition of the residual solid was confirmed to be a $Zn(DMTC)_2$ unit plus 2 equiv of NH_2Oct (Figure 2c, which is very similar to Figure 1f). The simple NMR spectrum suggested the formation of a symmetric intermediate (intermediate **II**; Figure 2c, lower panel) that resulted from the reaction between the two coordinated octylamines and the most electron-deficient thiocarbonyl carbons of the alkyldithiocarbamate ligands. On the other hand, the NMR spectrum of the solid isolated from the toluene solution of $Zn(DMTC)_2 \cdot 2NH_2Oct$ heated at 80 °C (Figure 2b) showed two different peaks corresponding to $-N(CH_3)_2$ at 3.12 and 3.41 ppm in DMSO-d_6, arising from an asymmetric structure (intermediate **I**; Figure 2b, lower panel) inferred to contain an unreacted DMTC ligand and a DMTC ligand that had reacted with octylamine. The relative intensities of the two $-N(CH_3)_2$ peaks changed with the heating time, and finally, the spectrum resembled that of the symmetric structure isolated in the

(29) Bell, N. A.; Johnson, E.; March, L. A.; Marsden, S. D.; Nowell, I. W.; Walker, Y. *Inorg. Chim. Acta* **1989**, *156*, 205–211.

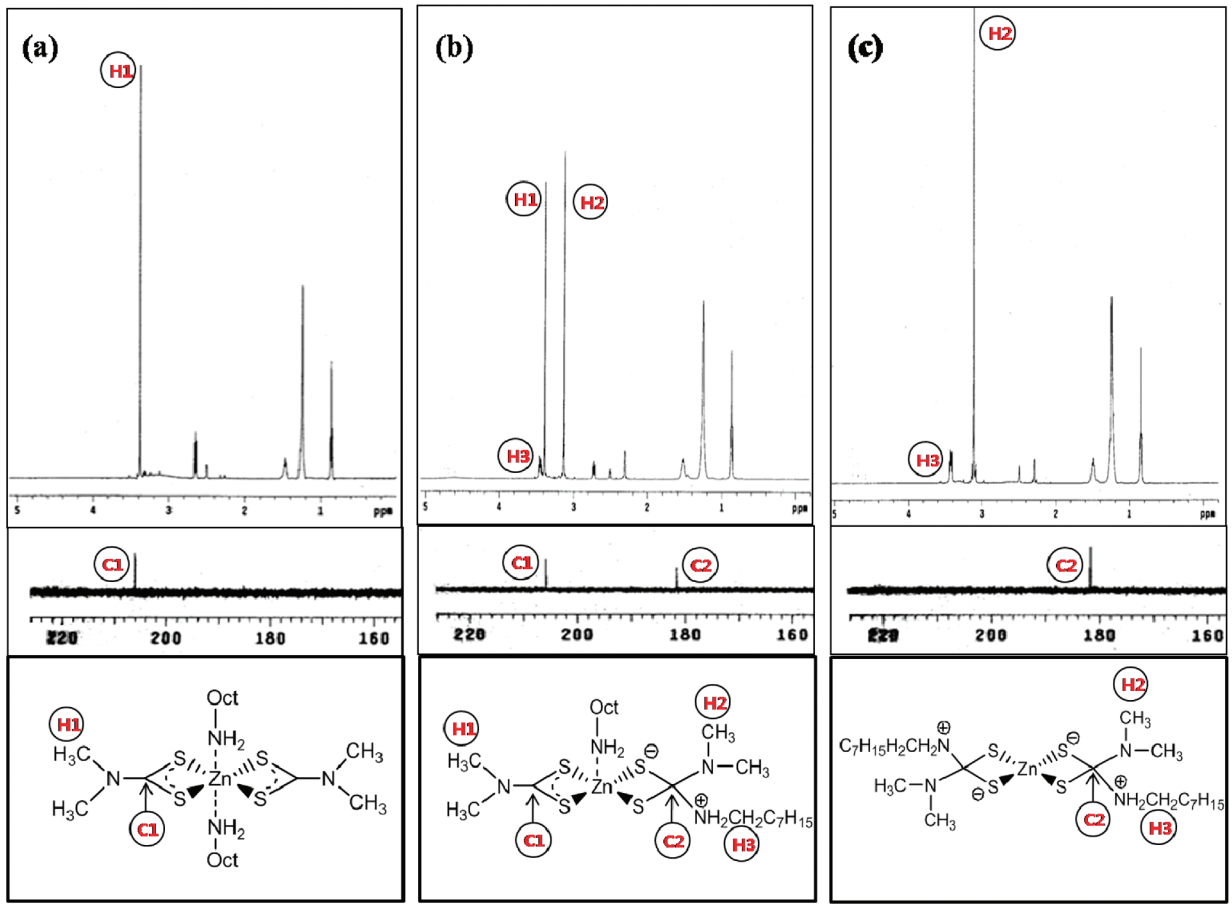

Figure 2. NMR spectra of $Zn(DMTC)_2 \cdot 2NH_2Oct$ after heating for 60 min at (a) 50, (b) 80, and (c) 100 °C.

experiment conducted at 100 °C. It is possible that the sample obtained from the experiment conducted at 80 °C was a simple mixture of hexacoordinated $Zn(DMTC)_2 \cdot 2NH_2Oct$ and fully converted symmetric intermediate **II** obtained by the consecutive migration of the two coordinated octylamines to the DMTC ligands. However, it is speculated that the structural change proceeds in a stepwise manner via the formation of the asymmetric intermediate **I**, as suggested in Figure 2b. Two peaks (at 207 and 182 ppm) corresponding to the thiocarbonyl carbon were detected in the ^{13}C NMR spectrum of intermediate **I** in DMSO-d_6. However, only one peak was detected in the ^{13}C NMR spectra of hexacoordinated $Zn(DMTC)_2 \cdot 2NH_2Oct$ (at 207 ppm) and fully converted symmetric intermediate **II** (at 182 ppm).

Single-crystal X-ray crystallography would have been useful in resolving the absolute configurations of the obtained intermediates. However, we were unable to prepare good-quality crystalline solids for this purpose. This was probably because intermediates **I** and **II** were structurally similar and unstable in the solution during recrystallization, even at room temperature for a long period of time.

We used two-dimensional (2D) NMR inverse C−H correlation techniques such as gradient heteronuclear single-quantum correlation (gHSQC; $^nJ_{C-H}$ with $n = 1$) and gradient heteronuclear multiple-bond correlation (gHMBC; $^nJ_{C-H}$ with $n = 2$, 3) to observe the thiocarbonyl carbon peaks with respect to the proton peaks in the spectra and thereby confirmed the structures of intermediates **I** and **II**. The gHSQC spectrum is used to determine the C−H connectivity involving direct C−H coupling. Therefore, the spectrum cannot provide any information regarding the nonprotonated thiocarbonyl carbon center, and unambiguous structural assignments cannot be made when the proton resonances exactly overlap. On the other hand, the gHMBC spectra help determine long-range or multiple-bond correlation, i.e, the correlation between a given carbon and the protons on the nearest two or three neighboring carbon atoms.

There are no cross-peaks in the gHSQC spectra of intermediates **I** and **II** because protons are not directly attached to the thiocarbonyl carbon (data not shown). However, there are several cross-peaks in the gHMBC ($J_{C-H} = 8$ Hz) spectra of intermediates **I** and **II**. These are due to the long-range coupling between the thiocarbonyl carbon and the protons of the neighboring dimethylamine and octylamine moieties (Figure 3). The spectrum of intermediate **I**, which was obtained at 80 °C, shows a cross-peak due to the C1−H1 correlation between the protons of the $-N(CH_3)_2$ group (3.40 ppm) and the thiocarbonyl carbon (207 ppm). Another set of cross-peaks, one corresponding to the C2−H2 correlation between the protons from $-N(CH_3)_2$ (3.10 ppm) and the reacted thiocarbonyl carbon (182 ppm) and the other to the C2−H3 correlation between the protons from $-NH_2CH_2C_7H_{15}$ (3.55 ppm) and the reacted thiocarbonyl carbon, also appear (Figure 3a). However, the spectrum of intermediate **II**, which was obtained at 100 °C, shows only two cross peaks, C2−H2 and C2−H3, because of its symmetric structure, which is attacked from both sides by the octylamine nucleophiles (Figure 3b).

These structures of intermediates **I** and **II** suggested from the NMR experiments are generated by the nucleophilic attack

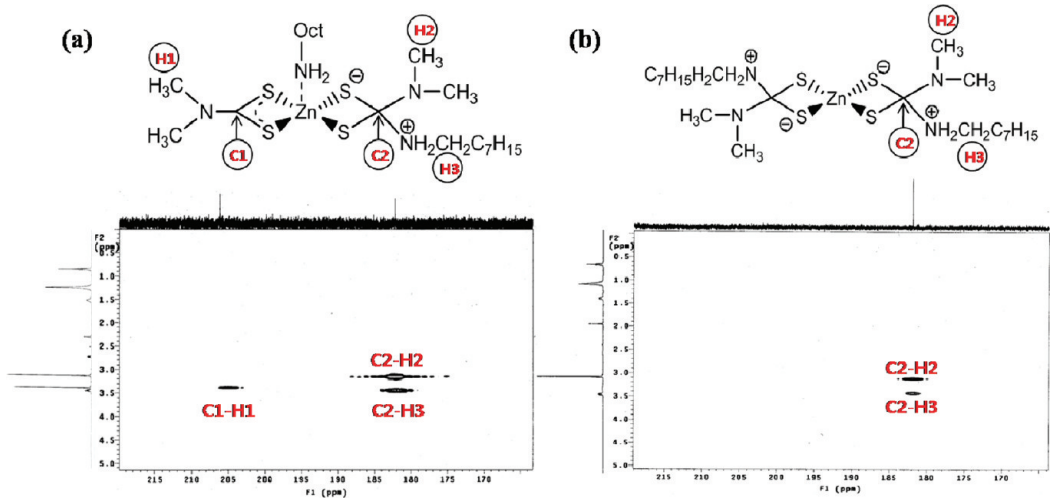

Figure 3. 2D NMR spectra from gHMBC experiments for (a) intermediate **I** and (b) intermediate **II**.

Scheme 1. Proposed Thermal Decomposition Mechanism of $Zn(DMTC)_2$ in the Presence of Octylamine To Form ZnS Nanoparticles in Three Steps: Intermediate Formation (Step 1), Decomposition To Release Thiourea (Step 2), and Condensation To Make the Zn−S−Zn Linkage (Step 4); Step 3 Shows the Amine Exchange Reaction

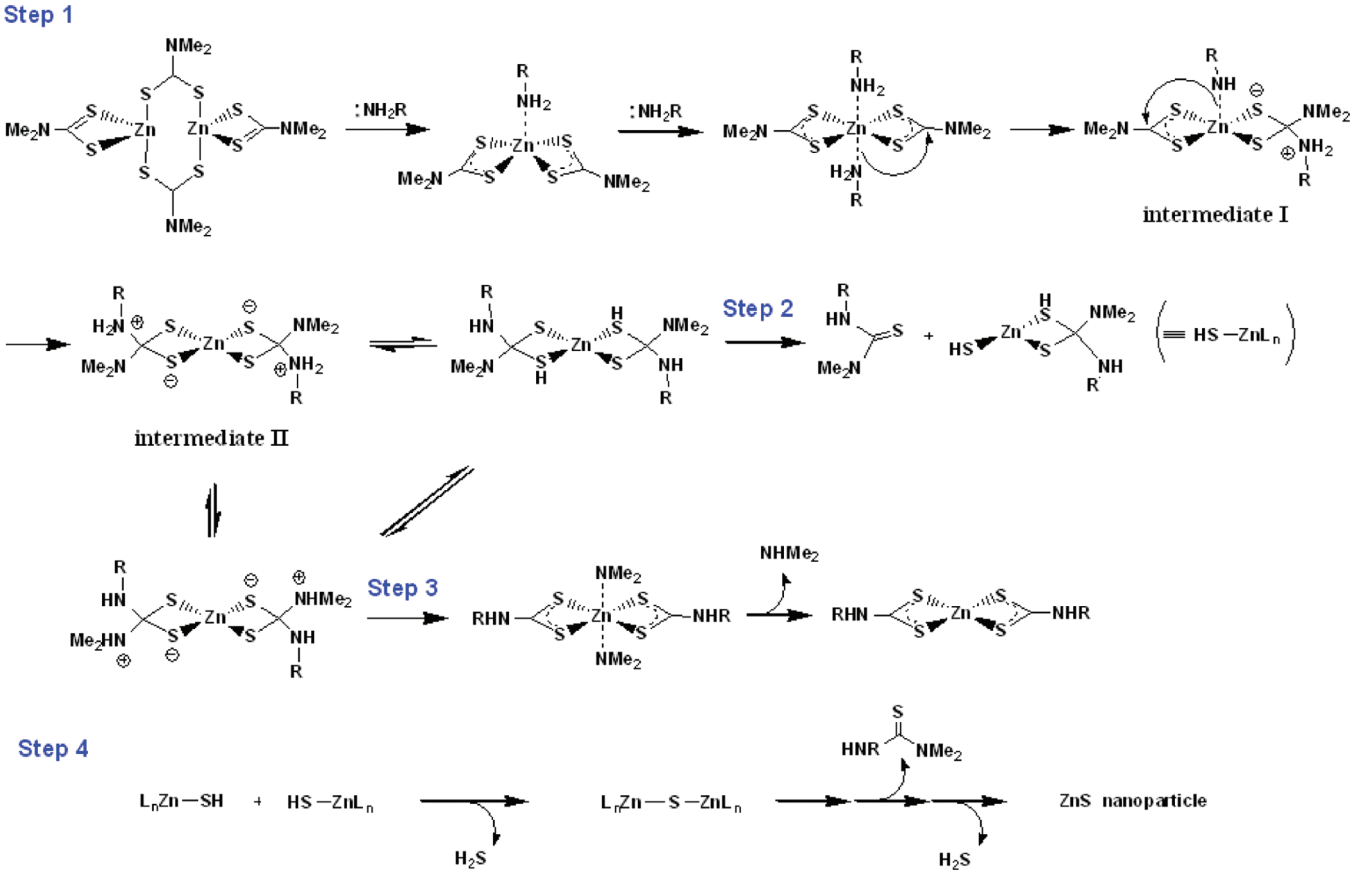

of the lone-pair electrons of nitrogen (from the coordinated octylamine) on the most electron-deficient thiocarbonyl carbon of the $Me_2N-CS_2^-$ ligand in $Zn(DMTC)_2$; this process is described in Scheme 1. $Zn(DMTC)_2$ has been known to form a tetrahedral structure with D_{2d} symmetry in the gas phase[30] and a dimeric structure in the crystal having a pseudotetrahedral coordination sphere around the zinc atoms, with each zinc atom bound to one chelating DMTC ligand and two bridging DMTC ligands.[31] In solutions containing coordinating ligands such as amines and carboxylate ions, pentacoordinated complexes are generated, as reported in the literature.[24,29,32] The results of the

(30) Hagen, K.; Holwill, C. J.; Rice, D. A. *Inorg. Chem.* **1989**, *28*, 3239–3242.

(31) Klug, H. P. *Acta Crystallogr.* **1966**, 536–546.

(32) McCleverty, J. A.; Spencer, N.; Bailey, N. A.; Shackleton, S. L. *J. Chem. Soc., Dalton Trans.* **1980**, 1939–1944.

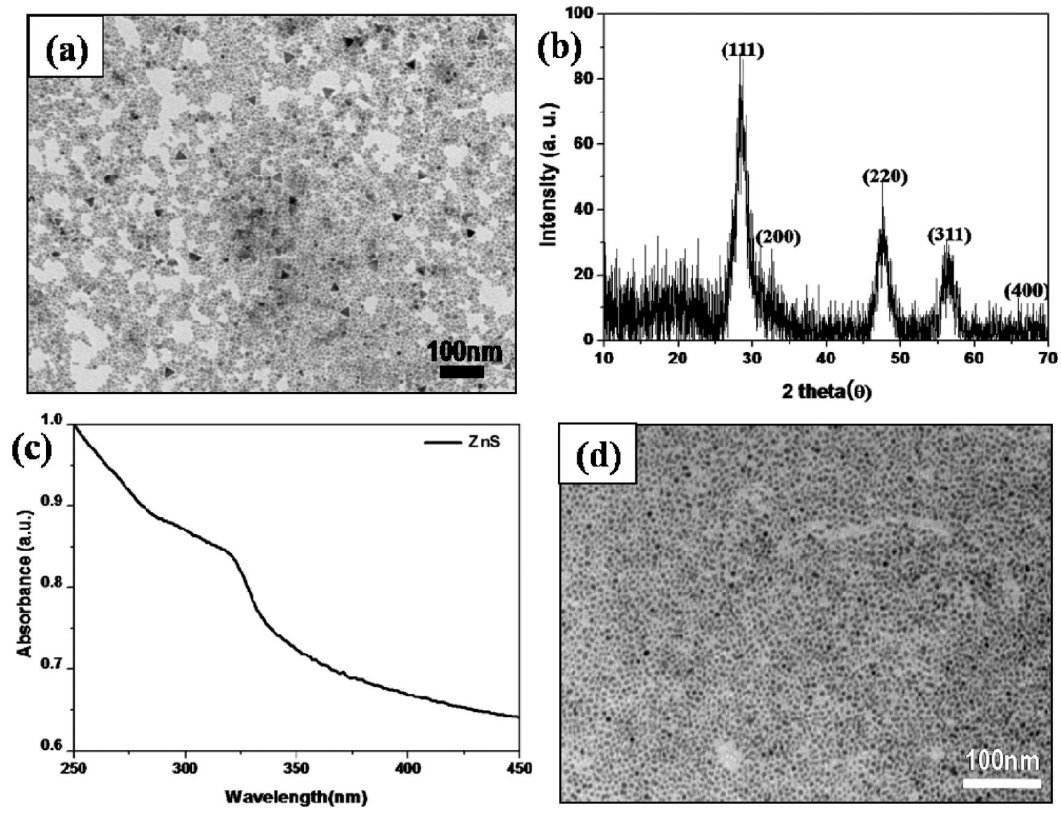

Figure 4. (a) TEM image, (b) XRD pattern, and (c) UV−vis absorption spectrum (in hexane) of the solid precipitate obtained by thermal decomposition of $Zn(DMTC)_2$ in the presence of octylamine. (d) TEM image of the solid precipitate generated when oleic acid was added as a capping ligand.

above-mentioned NMR analyses suggest that 2 equiv of octylmaine binds to $Zn(DMTC)_2$ to generate penta- and hexacoordinated complexes in solution. With an increase in temperature, the coordinated octylamines migrate to the most electron-deficient thiocarbonyl carbons of the dialkyldithiocarbamate ligands to generate the asymmetric intermediate **I** at 80 °C and the symmetric intermediate **II** at a higher temperature of ∼100 °C (step 1 in Scheme 1). Through proton migration, intermediate **II** is in equilibrium with a neutral form, which generates $HS-ZnL_n$ by releasing *N*-octyl-*N*′,*N*′-dimethylthiourea (step 2 in Scheme 1). Upon condensation of $HS-ZnL_n$, Zn−S−Zn linkages are formed, and H_2S is released. Hence, $HS-ZnL_n$ can be regarded as a building block of ZnS nanoparticles. ZnS nanoparticles are produced by the consecutive decompositions of the amine-inserted dithiocarbamate ligands accompanied by the condensation of $HS-ZnL_n$ (step 4 in Scheme 1).

The colorless solution of $Zn(DMTC)_2$ and 2 equiv of octylamine turned yellow upon heating. This was accompanied by gas evolution and the formation of a pale-yellow precipitate. The organic side product in the supernatant was confirmed to be pure *N*-octyl-*N*′,*N*′-dimethylthiourea by NMR spectroscopy and fast-atom-bombardment MS (FAB-MS) (Figure S1 in the Supporting Information). The evolved gas was trapped using an aqueous Pb^{2+} solution to form a black precipitate of PbS; this confirmed that the gas was H_2S (Figure S2 in the Supporting Information). By TEM, XRD, and UV−vis spectroscopy, the pale-yellow precipitate obtained in the thermal reaction of $Zn(DMTC)_2$ with 2 equiv of octylamine was confirmed to be ZnS nanoparticles (Figure 4). The average size of these ZnS nanoparticles was on the order of a few nanometers. The ZnS nanoparticles had a broad size distribution because they were synthesized in the absence of a sufficient amount of capping ligand and appropriate size control (Figure 4a). The thermal reaction of $Zn(DMTC)_2$ with 2 equiv of octylamine in the presence of oleic acid, a capping ligand, afforded uniformly sized ZnS nanoparticles (Figure 4d).

It is also possible that the protons of intermediate **II** migrate to the $-N(CH_3)_2$ group instead of the coordinated sulfur, thereby resulting in an amine exchange reaction (step 3 in Scheme 1). This reaction is similar to the transamidation reaction of carboxyamides with amines, which proceeds only in the presence of Lewis acid catalysts such as organometallic complexes of Al(III) or Ti(IV).[33−35] A small amount of exchanged dimethylamine, $HN(CH_3)_2$, was detected at ∼2.3 ppm in the VT-NMR spectrum of $Zn(DMTC)_2 \cdot 2NH_2Oct$ (Figure 1), and the generation of $HN(CH_3)_2$ was clearly detected in the spectra of the solid intermediates at 2.3 ppm (Figure 2b,c). The rate of thermal decomposition of $Zn(DMTC)_2$ in the presence of excess octylamine increased, as reported for common pyrolysis reactions in the literature, and *N*,*N*′-dioctylthiourea (symmetric thiourea) was obtained instead of *N*-octyl-*N*′,*N*′-dimethylthiourea (asymmetric thiourea) as the organic side product in the supernatant. In the presence of excess octylamine, transamidation (step 3 in Scheme 1) afforded $Zn(S_2CNHOct)_2$ and/or its dimeric form, which could be coordinated with the excess octylamine to generate a new hexacoordinated structure, as shown below:

(33) Eldred, S. E.; Stone, D. A.; Gellman, S. H.; Stahl, S. S. *J. Am. Chem. Soc.* **2003**, *125*, 3422–3423.
(34) Hoerter, J. M.; Otte, K. M.; Gellman, S. H.; Stahl, S. S. *J. Am. Chem. Soc.* **2006**, *128*, 5177–5183.
(35) Kissounko, D. A.; Hoerter, J. M.; Guzei, I. A.; Cui, Q.; Gellman, S. H.; Stahl, S. S. *J. Am. Chem. Soc.* **2007**, *129*, 1776–1783.

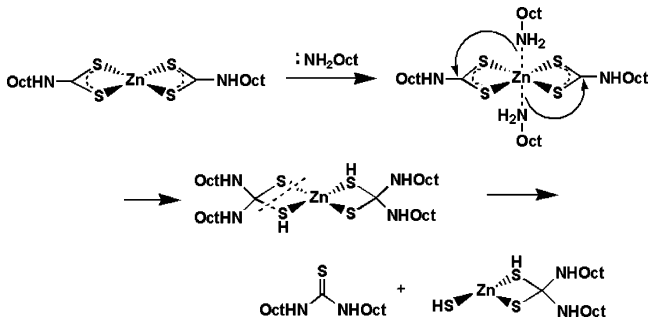

Consecutive decomposition of the hexacoordinated structure (similar to step 2 in Scheme 1) yielded symmetric *N*,*N*′-dioctylthiourea.

The average size of the ZnS nanoparticles generated from the different reaction conditions using various amount of octylamine clearly showed the effect of thermal decomposition kinetics. Even though the size distribution and the shape regularity were not ideal for comparison with those for the nanoparticles generated in the presence of the capping ligand (oleic acid), the size of the generated ZnS nanoparticles tended to decrease as the amount of octylamine increased. The average sizes of the ZnS nanoparticles from the reactions with 2 and 5 equiv of octylamine were measured as 6 ± 2 and 3 ± 1 nm, respectively (Figure S3 in the Supporting Information). When 10 equiv of octylamine was used, the shape of generated ZnS was changed to elongated sphere and nanorod forms (average diameter of nanorod: 3 ± 1 nm, length: 10 ± 4 nm). The absorption spectra of these ZnS nanomaterials also showed that the absorption maxima shifted to higher energy when a large amount of octylamine was used to accelerate the decomposition reaction (Figure S4 in the Supporting Information). These results could be explained by the fact that the rate of thermal decomposition of $Zn(DMTC)_2$ was accelerated in the presence of the excess amount of octylamine to generate a larger number of seeds and produce smaller-sized nanoparticles, and the shape of ZnS nanomaterials were not well-controlled in the absence of a surface-stabilizing (capping) ligand such as oleic acid.

Thiourea, H_2S, and ZnS nanoparticles were not obtained when a secondary amine such as dioctylamine ($HNOct_2$) was used instead of the primary amine octylamine in the decomposition of $Zn(DMTC)_2$. In this case, only $HN(CH_3)_2$ was obtained, and $Zn(DMTC)_2$ was converted to $Zn(S_2CNOct_2)_2$ through the previously mentioned amine exchange reaction. This was probably due to the steric hindrance around the thiocarbonyl carbon. This steric hindrance could cause an unfavorable steric interaction when a proton is in close proximity to the lone pair of the sulfur atom (to prevent the decomposition represented by step 2 in Scheme 1) while causing a favorable proton migration to the $-N(CH_3)_2$ group (to enable the amine exchange reaction shown in step 3 in Scheme 1). More precise calculations and experiments are required to confirm the proposed decomposition mechanism. However, the results obtained from another control experiment supported this hypothesis. A Zn complex having a primary amine unit on the dithiocarbamate ligand, $Zn(S_2CNHOct)_2$, could react with dioctylamine (a secondary amine) and decompose into asymmetric *N*-octyl-*N*′,*N*′-dioctylthiourea, H_2S, and ZnS nanoparticles (Figure S5 in the Supporting Information).

The proposed mechanism of the amine-promoted thermal decomposition reactions of zinc dithiocarbamate precursor complexes can be extended to other metals such as lead and cadmium. DETC was used to prepare lead and cadmium complexes, and their decomposition reactions with octylamine at 100 °C were monitored. As expected, asymmetric *N*-octyl-*N*′,*N*′-diethylthiourea was detected in the supernatant, and CdS (10−15 nm) and PbS (200−500 nm) nanoparticles were obtained (Figures S6 and S7 in the Supporting Information). The size of the obtained nanoparticles appeared to be related to the relative stability of the precursor metal complexes. Since the average sizes of Pb^{2+}, Cd^{2+}, and Zn^{2+} are 133, 109, and 88 pm, respectively, in their hexacoordinated complexes,[36] the stabilities of these complexes are expected to be in the following order: $Pb(DETC)_2 < Cd(DETC)_2 < Zn(DMTC)_2$. The rate of the decomposition reaction was well-consistent with the aforementioned trend.

The critical role of the amine in the thermolysis method used for the synthesis of metal sulfide nanoparticles could be extended to the synthesis of metal oxide (MO_x) nanoparticles as well. A study of the thermolysis of cadmium oleate to afford CdO nanoparticles revealed that the decomposition temperature in the presence of octylamine was ∼50 °C lower than that in the absence of octylamine. The organic side product isolated from the supernatant was found to be octyl oleylamide. Detailed studies must be carried to confirm the decomposition mechanism. However, on the basis of our proposed decomposition mechanism and in view of the major role of amines in decomposition, we speculate that thermal decomposition could be extended to many interesting applications, such as the synthesis of nanomateials within a selected area for patterning and generation of alloy nanoparticles through consecutive thermolysis.

Conclusions

We have investigated the mechanism underlying amine-promoted thermal decomposition of single-molecule precursors, namely, zinc alkyldithiocarbamate complexes, in order to understand the conversion of the precursor molecules into intermediates, their decomposition into nanoparticles, and the critical role of the amine in the process. Nucleophilic attack of the coordinated amine on the electron-deficient thiocarbonyl carbon of the alkyldithiocarbamate ligand is the first step in the decomposition of zinc alkyldithiocarbamate complexes. NMR and MS studies of the organic side products generated from different alkylamines at various concentrations have revealed that steric hindrance in the alkylamine is very critical to the rate of decomposition of the zinc alkyldithiocarbamate complexes and the competitive reaction pathways involving the intermediates.

The proposed mechanism of the amine-promoted thermal decomposition of zinc dithiocarbamate precursor complexes could be extended to the synthesis of metal sulfide and metal oxide nanoparticles from other metal precursor complexes; further research must be carried out to confirm this mechanism.

Acknowledgment. This work was supported by a Korea Science and Engineering Foundation (KOSEF) grant funded by the Korean Government (MEST, R01-2008-000-20302-0). Y.K.J. and J.I.K. gratefully acknowledge the BK21 Fellowship.

Supporting Information Available: Detailed characterization data of metal sulfide nanoparticles and related side products from the thermal decomposition reactions by NMR, MS, TEM, and XRD. This material is available free of charge via the Internet at http://pubs.acs.org.

JA905353A

(36) Shannon, R. D. *Acta Crystallogr.* **1976**, *A32*, 751–767.